



# DAMAGE EVOLUTION IN THE SHORT FIBRE REINFORCED COMPOSITE STRUCTURES

Evgeny V. Morozov

The University of New South Wales Asia, Singapore

**Keywords:** *Progressive Failure, Damage Modelling, Crash Simulation, SMC Composites*

## Abstract

*The paper is concerned with the computational progressive damage material modelling and numerical simulation of impact response of thin-walled composite structures made from SMC (sheet moulding compound) polymer composites reinforced with randomly oriented short fibres.*

*The development of an appropriate way of modelling and computational analysis of the failure evolution in the thin-walled composite components with complex geometries is one of the primary goals of the research.*

*The findings are applied through the development and implementation of a customized material failure model using the explicit finite element code (PAM-CRASH). The proposed methodology involves experimental material characterisation and application of a finite element material degradation model to simulate dynamic loading situations. The failure models and simulation methods are validated by comparing numerical results with experimental data.*

## 1 Introduction

The design and implementation of new composite structural components (body panels, bumpers, crash absorbers, etc.) in aerospace and automotive applications requires the development of new approaches to structural analysis. This should be based on the utilization of advanced modelling and simulation technologies.

The progressive damage model development for SMC (sheet moulding compound) composites and its implementation into the finite element software package (PAM-CRASH) are presented in this paper. To predict and refine the safety characteristics of aerospace and automotive composite structural components, a demand has arisen for material models capable of producing simulations with these materials [1]. The SMC composites under consideration represent one of the groups of short fibre reinforced composite materials.

At present, an examination of the most commonly used software packages in the field of structural crashworthiness reveals that composite material models are limited to the family of continuously reinforced long-fibre composites. Dedicated models for the simulation of short-fibre composites are lacking. The present work addresses this issue with an investigation into the behaviour of the short fibre reinforced materials and structures. The development of an appropriate way of modelling and computational analysis of the dynamic behaviour of thin-walled SMC composite components with complex (mixed) geometries is the main purpose of the present work.

The adopted methodology involves the implementation of specific dynamic analysis and design software tools, progressive damage model development and material characterisation. The approach developed in the present work is based on the direct approximation of the macro-mechanical behaviour of composite material presented in the form of stress-strain curves obtained from the macroscopic material characterisation tests. The paper demonstrates this approach for the crush simulation of the scaled down automotive composite component. The failure development is modelled using an explicit finite element code.

The failure models and simulation methods are validated by comparing numerical results with experimental data which are obtained from the mechanical testing of the thin-walled composite components manufactured from SMC composite.

## 2 Damage Evolution Modelling

Successful micro-mechanical models in the range of short fibre reinforced composites exist and have been applied to uni-axial tensile simulations [2-5]. These models investigate micro-mechanical failure modes through microscopic testing, revealing damage mechanisms such as matrix micro-cracking, interfacial debonding, fibre pull-out, fibre breakages and pseudo-delamination. These failures are then

applied to the material as a whole to determine the macroscopic effect. Any review of modelling trends will immediately show a distinct division between those models that are theoretically based, using mathematical formulations to relate the material properties of the overall composite material to those of more simply characterized constituents, and those that are based strongly on experimental testing and data of the composite as a material [2-5]. Typically, micro-mechanical models would require the implementation of sophisticated experimental testing (sometimes impractical and expensive) in order to characterize the material constituents and their interactions. Moreover, most of the micromechanical models could hardly be used for practical analysis of composite materials and structures. The reason for this is that irrespective of how rigorous the micromechanical model is, it cannot describe adequately enough real material microstructure and take into account voids, micro-cracks, randomly damaged or misaligned fibres and many other effects. For this reason, micro-mechanical models are mostly used for qualitative analysis. The approach taken here differs to this by only considering the macro-mechanical behaviour of the material from stress-strain results of macroscopic material characterization tests. Focus is rather applied to developing a simplified practical methodology to characterise a short fibre reinforced composite and then apply this through a material model to simulate damage evolution. The research operates under the hypothesis that the SMC material is relatively homogeneous and isotropic.

The modelling is based on the direct approximation of the experimental stress-strain curve for given SMC composite material. This is combined with the finite element incremental technique where the stiffness of each element is degraded as the stress and strain level increases resulting in a damage mechanics law. Each shell element has a set number of calculation points ( $i$ ) located through the thickness at its centre. Within the PAM-CRASH explicit code, the stresses at each calculation point ( $i$ ) during cycle  $n$  are calculated as follows:

$$\{\sigma\}_n^{(i)} = [\mathbf{C}]_n^{(i)} \{d\varepsilon\}_n^{(i)} + \{\sigma\}_{n-1}^{(i)} \cdot FAIL_{n-1}^{(i)} \quad (1)$$

where

$$\begin{aligned} \{\sigma\}_n^{(i)} &= \{\sigma_{11}, \sigma_{22}, \tau_{12}, \tau_{13}, \tau_{23}\}^T \\ \{d\varepsilon\}_n^{(i)} &= \{d\varepsilon_{11}, d\varepsilon_{22}, d\gamma_{12}, d\gamma_{13}, d\gamma_{23}\}^T \\ &\text{(the incremental strains at cycle } n), \end{aligned}$$

and  $[\mathbf{C}]_n^{(i)}$  is the stiffness matrix, whereas

$$\{\sigma\}_{n-1}^{(i)} = \{\sigma_{11}, \sigma_{22}, \tau_{12}, \tau_{13}, \tau_{23}\}_{n-1}^T$$

are the stresses at cycle  $n-1$  (time step  $\Delta t$ ).

The material degradation law is introduced by altering the material properties at each of the calculation points. A damage parameter  $DAM$  is introduced as a measure of the macroscopic isotropic damage in the composite. The new stiffness matrix is calculated as follows:

$$[\mathbf{C}]_n^{(i)} = [\mathbf{C}] \cdot DAM_{n-1}^{(i)} \quad (2)$$

where  $[\mathbf{C}]$  is the original stiffness matrix for the undamaged material

$$[\mathbf{C}] = \begin{bmatrix} \frac{E}{1-\nu^2} & \frac{\nu E}{1-\nu^2} & 0 & 0 & 0 \\ \frac{\nu E}{1-\nu^2} & \frac{E}{1-\nu^2} & 0 & 0 & 0 \\ 0 & 0 & \frac{E}{2(1+\nu)} & 0 & 0 \\ 0 & 0 & 0 & \frac{\kappa E}{2(1+\nu)} & 0 \\ 0 & 0 & 0 & 0 & \frac{\kappa E}{2(1+\nu)} \end{bmatrix}$$

where  $E$  is Young's modulus,  $\nu$  is Poisson's ratio and  $\kappa$  is the shear factor.

The parameter  $DAM$  equals 1 for an undamaged state, and degrades towards zero as stress and strain increases. The von Mises failure criterion is employed at this stage of the development to determine the stress levels where degradation occurs.

A failure parameter  $FAIL$  is introduced as an indicator of whether the material has completely failed at a calculation point, and thus lost all or the majority of load-carrying ability ( $FAIL$  is equal to 1 for intact material and 0 for failure). Calculation of stresses at failure varies depending on the stress-strain relation. The stress can be stepped to zero as the material fails, or some residual value of stress can be held.

Experimental material characterisation has been applied to define the levels at which degradation and failure occurred. This involves tensile/compressive material testing to produce stress-strain graphs. Data points are then extracted from these graphs to obtain the values of  $DAM$  and  $FAIL$  for different intervals of stress and strain.

The proposed model has been implemented as the material definition subroutine in the PAM-CRASH software package.

The damage law definition based on the direct approximation of the stress-strain curves could be performed using tensile or compressive tests or the results of both. For the latter the appropriate strength criterion capable to take into consideration the differences in composite behaviour under tension and compression should be employed.

The way of the introduction of the damage law is demonstrated for the stress-strain curves obtained from the tensile tests (see Fig. 1). The SMC composite material under consideration has been reinforced with glass fibres of length 25mm with a volume fraction  $V_f = 20\%$  randomly oriented in a polyester resin matrix [6-7].

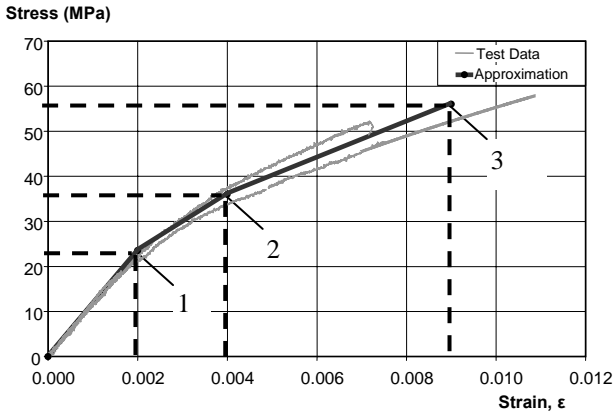


Fig. 1. Material characterization using stress-strain diagram

The approximation of the experimental stress-strain curves provides the basis for the damage law definition. The approximated curve was divided into three piecewise linear regions with the understanding that the number of the linear sections of the curve could be increased if necessary to provide a closer approximation of the experimental results [8].

The values of stress and strain at the three points indicated in Fig. 1 were extracted as follows:

$$\sigma_{L1} = 23.54 \text{ MPa}, \quad \varepsilon_{L1} = 0.002$$

$$\sigma_{L2} = 36 \text{ MPa}, \quad \varepsilon_{L2} = 0.004$$

$$\sigma_{L3} = 56 \text{ MPa}, \quad \varepsilon_{L3} = 0.009$$

where  $\sigma_L$  and  $\varepsilon_L$  are the stress and the corresponding strain limits respectively. The moduli (slopes of the stress-strain curve) between these points are then calculated as:

$$E_1 = \frac{\sigma_{L1}}{\varepsilon_{L1}} = 11.77 \text{ GPa},$$

$$E_2 = \frac{\sigma_{L2} - \sigma_{L1}}{\varepsilon_{L2} - \varepsilon_{L1}} = 6.23 \text{ GPa},$$

$$E_3 = \frac{\sigma_{L3} - \sigma_{L2}}{\varepsilon_{L3} - \varepsilon_{L2}} = 4.00 \text{ GPa}$$

The damage law is introduced by calculating  $DAM$  as the factor by which the slope of the stress-strain curve is decreased at points 1 and 2 from its original value. The stiffness matrix is then multiplied by this factor to initiate the degradation of the material. At point 3, the failure parameter is set to zero and subsequently all stresses drop to zero in the next time step. The corresponding damage law at calculation point  $i$ , cycle  $n$  for is presented in the following form:

$$DAM_0^{(i)} = FAIL_0^{(i)} = 1 \text{ (at cycle 0)}$$

$$[C]_n^{(i)} = [C] \cdot DAM_{n-1}^{(i)} \quad (3)$$

$$\{\sigma\}_n^{(i)} = [C]_n^{(i)} \{d\varepsilon\}_n^{(i)} + \{\sigma\}_{n-1}^{(i)} \cdot FAIL_{n-1}^{(i)}$$

If  $VM_n > \sigma_{L1}$  and  $DAM_{n-1} = 1$ , then

$$DAM_n = \frac{E_2}{E_1} = 0.53$$

If  $VM_n > \sigma_{L2}$  and  $FAIL_{n-1} = 1$ , then (4)

$$DAM_n = \frac{E_3}{E_1} = 0.34$$

If  $VM_n > \sigma_{L3}$  then

$$DAM_n = 0 \quad \text{and} \quad FAIL_n = 0$$

This type of model parameters is used as the input data for the material definition subroutine.

### 3 Crush testing and simulation

Implementation of the model is based on the use of the PAM-CRASH user-defined material template, Material 180 [8-9]. The material behaviour is defined in terms of stress-strain calculations in the material definition subroutine, written in FORTRAN coding. The subroutine is divided into three sections: input, solver and auxiliary output. Apart from coding the damage law under consideration into the solver section, the input section is altered to accept the material properties and parameters specific to the

new model. Outputs of the von Mises stress, *VM* and the damage and failure parameters, *DAM* and *FAIL* are calculated in the auxiliary outputs section. Once coding is complete, the subroutine is compiled with the main PAM-CRASH code yielding a new executable solver program. Under normal operation (with no user-defined materials), the PAM-CRASH simulation process begins with constructing the simulation input (preparing the mesh, stipulating materials, setting boundary and loading conditions and setting simulation parameters). This is saved into a simulation input file, which is then posed to the solver program. Once calculation is complete, results are viewed and post-processed.

In order to test the validity of the material model, simulations of a complex loading test are compared with experimental results. The test chosen is the crushing of a scaled-down automotive spare-wheel compartment made from SMC composite material (see Fig. 2).

Scaling of the structural prototype has been predetermined by the power and size of working area of available testing rig.

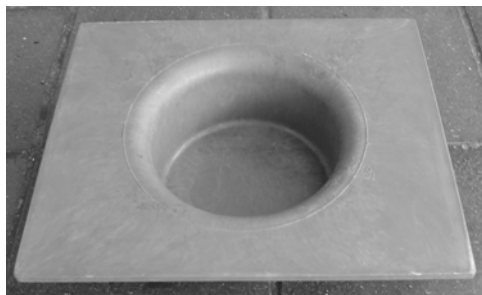


Fig. 2. SMC composite component

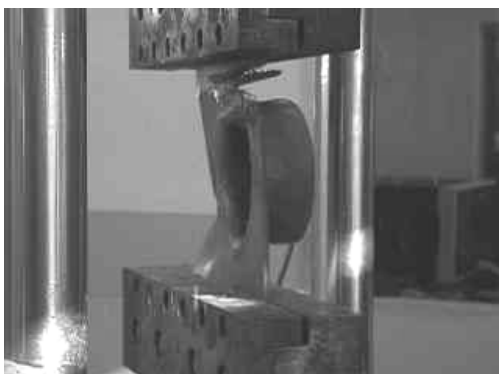


Fig. 3. Crushing test setup

The test prototype was scaled down to 230x190 mm, with the wheel well diameter of 120 mm, depth of 50 mm and a uniform thickness of 4 mm. The test setup is shown in Fig. 3.

The components have been crushed under compressive loading at speeds of 2, 50, 100 and 330 mm/s using a hydraulic MTS test rig. A set of force-displacement curves and video footage was produced for the same SMC composite material [9]. The experimental force-displacement curves are shown in Figs. 4 and 9.

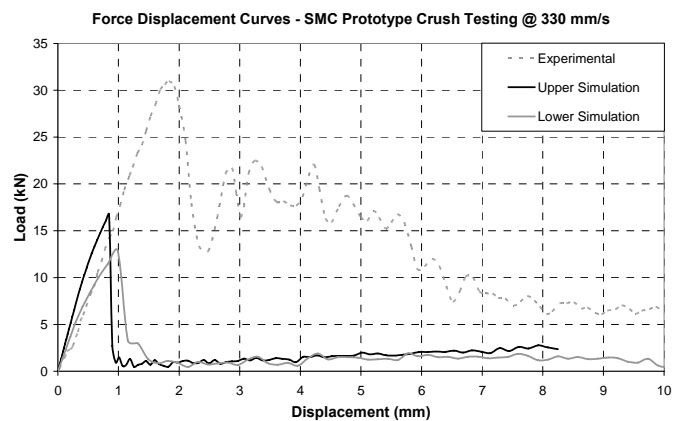


Fig. 4. Crush testing and simulation results

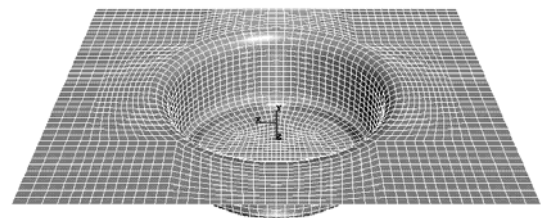


Fig. 5. Meshed model of the component

The geometry of prototype was chosen due to its complexity, incorporating both flat and cylindrical portions. The meshed prototype component is shown in Fig. 6. The three rows of elements on either side represent the clamps, constrained as rigid bodies in PAM-CRASH. Loading was applied by setting a displacement boundary condition to the centre-of-gravity of one clamp, and fixing the other. The moving clamp was given two degrees of freedom, viz. the translation in the axial direction of loading and rotation about this axis (in the experimental setup the moving clamp could rotate about its axis of translation). To compare simulated and experimental results, an output of the force through the clamps was requested. PAM-CRASH also produces an animation where colour coded contours of the von

Mises stress and damage and failure parameters can be applied.

Input parameters for numerical simulation were extracted as discussed in Section 2 from the tensile characterisation testing (see Fig. 6).

To investigate the sensitivity of the model to the selection of sample points, two approximations were used. The set of experimental tensile stress-strain curves (see Fig.1) is bounded by upper and lower limit curves. The input points were extracted from these two curves as shown in Fig. 6.

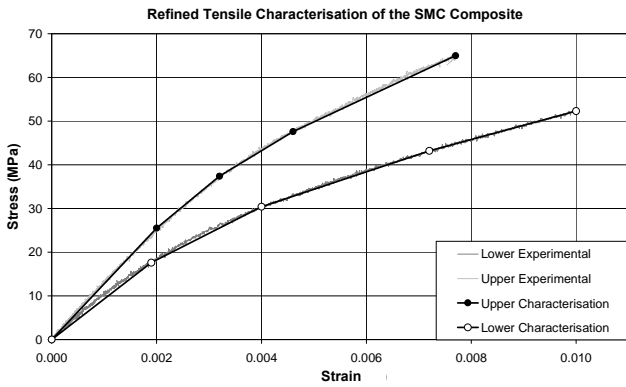


Fig. 6. Material characterization using tensile test results

The number of approximation points for the damage law representation was increased from three to four. For the upper curve, the properties at the limit points and corresponding moduli/slopes were extracted as:

$$\begin{aligned}\sigma_{L1} &= 25.5 \text{ MPa}, \quad \varepsilon_{L1} = 0.0020 \\ \sigma_{L2} &= 37.4 \text{ MPa}, \quad \varepsilon_{L2} = 0.0032 \\ \sigma_{L3} &= 47.6 \text{ MPa}, \quad \varepsilon_{L3} = 0.0046 \\ \sigma_{L4} &= 65.0 \text{ MPa}, \quad \varepsilon_{L4} = 0.0077\end{aligned}$$

$$\begin{aligned}E_1 &= 12.75 \text{ GPa}, \quad E_2 = 9.92 \text{ GPa}, \\ E_3 &= 7.29 \text{ GPa}, \quad E_4 = 5.61 \text{ GPa}\end{aligned}$$

The same was done for the lower curve:

$$\begin{aligned}\sigma_{L1} &= 17.6 \text{ MPa}, \quad \varepsilon_{L1} = 0.0019 \\ \sigma_{L2} &= 30.4 \text{ MPa}, \quad \varepsilon_{L2} = 0.0040 \\ \sigma_{L3} &= 43.2 \text{ MPa}, \quad \varepsilon_{L3} = 0.0072 \\ \sigma_{L4} &= 52.3 \text{ MPa}, \quad \varepsilon_{L4} = 0.0010\end{aligned}$$

$$\begin{aligned}E_1 &= 9.26 \text{ GPa}, \quad E_2 = 6.10 \text{ GPa}, \\ E_3 &= 4.00 \text{ GPa}, \quad E_4 = 3.25 \text{ GPa}\end{aligned}$$

To incorporate the fourth limit point, the conditions in the damage law, Eqs. (3)-(4), were altered:

$$\begin{aligned}\text{If } VM_n > \sigma_{L1} \text{ and } DAM_{n-1} = 1, \text{ then} \\ DAM_n = DAM_2 = \frac{E_2}{E_1} = 0.78 \text{ (upper)} \\ \text{and } 0.66 \text{ (lower)} \\ \text{If } VM_n > \sigma_{L2} \text{ and } DAM_{n-1} = DAM_2, \\ \text{then } DAM_n = DAM_3 = \frac{E_3}{E_1} = 0.57 \text{ (upper)} \quad (5) \\ \text{and } 0.43 \text{ (lower)} \\ \text{If } VM_n > \sigma_{L3} \text{ and } DAM_{n-1} = DAM_3, \\ \text{then } DAM_n = DAM_4 = \frac{E_4}{E_1} = 0.44 \text{ (upper)} \\ \text{and } 0.35 \text{ (lower)} \\ \text{If } VM_n \geq \sigma_{L4}, \text{ then } DAM_n = 0 \text{ and } FAIL_n = 0\end{aligned}$$

Simulations were performed for the 330 mm/s crushing test. The resulting simulated force-displacement curves are compared with the experimental results in Fig. 4.

As can be seen particularly in the force-displacement curves, the experimental and simulated profiles look alike at the initial stage of loading. However, the predicted peak load is lower and the failure after peak load occurs more rapidly, compared to the gradual descent of the experimental load curve. The sudden drop-off in load can be attributed to the catastrophic failure in the tensile characterisation (the drop of stress to zero after the fourth stress limit has been breached).

At the same time, the simulated failure modes and damaged areas (see Fig. 7) show reasonable agreement with experimental failure patterns.

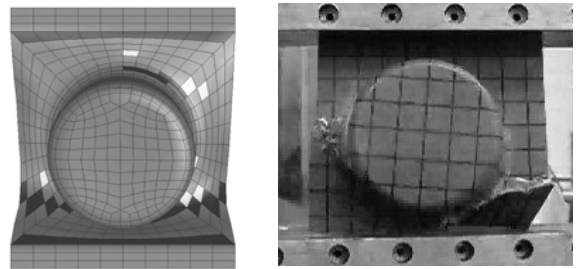


Fig.7. Comparison of the failure patterns: simulated vs. experimental.

The elements in the middle part of the component are eliminated at the peak load and the structure then

has no load-carrying ability apart from through the upper wheel-well section. In reality, the failure is not so drastic and these middle elements should still carry some load.

To address these issues related to the aforementioned discrepancies in the simulated and experimental results the computations have been performed using the model input data obtained from the compressive testing of the flat SMC material specimens. The corresponding experimental stress-strain characterisation curve is shown in Fig. 8. The damage law with three data points and a constant post-failure residual stress of 10 MPa has been used [8]. The limit points and corresponding moduli are

$$\begin{aligned} \sigma_{L1} &= 25.5 \text{ MPa}, \varepsilon_{L1} = 0.006 \\ \sigma_{L2} &= 74.1 \text{ MPa}, \varepsilon_{L2} = 0.0237 \\ \sigma_{L3} &= 113 \text{ MPa}, \varepsilon_{L3} = 0.044 \end{aligned}$$

$$E_1 = 4.25 \text{ GPa}, E_2 = 2.75 \text{ GPa}, E_3 = 1.92 \text{ GPa}$$

$$\begin{aligned} \sigma_{L1} &= 25.5 \text{ MPa}, \varepsilon_{L1} = 0.006 \\ \sigma_{L2} &= 74.1 \text{ MPa}, \varepsilon_{L2} = 0.0237 \\ \sigma_{L3} &= 113 \text{ MPa}, \varepsilon_{L3} = 0.044 \end{aligned}$$

$$E_1 = 4.25 \text{ GPa}, E_2 = 2.75 \text{ GPa}, E_3 = 1.92 \text{ GPa}$$

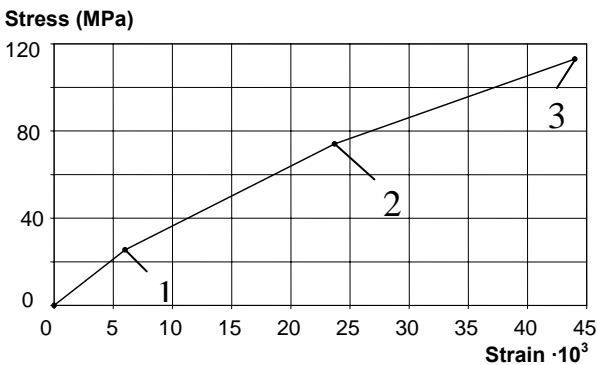


Fig. 8. Approximation of the compressive stress-strain curve and the model data points

The adoption of the catastrophic failure at the finite element level does not always provide a fully realistic representation of the material's behaviour under crushing. The elimination of elements based on this approach means that no load can be transmitted through these elements. This does not reflect the possibility when the material could be compacted together under compression and could still carry some load after failure. To address this, the residual stress of 10 MPa has been introduced in

order to reflect the ability of the material to carry load after failure due to the post-failure compaction.

The results from force-displacement curves and images of the damaged areas and failure modes are compared in Figs. 9 and 10.

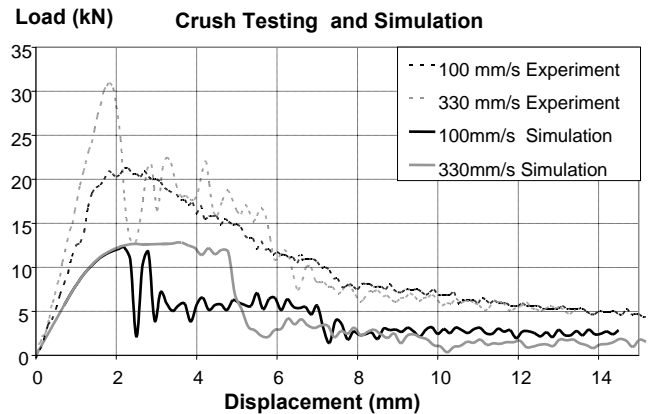


Fig.9. Force-displacement curves for crushing of Component

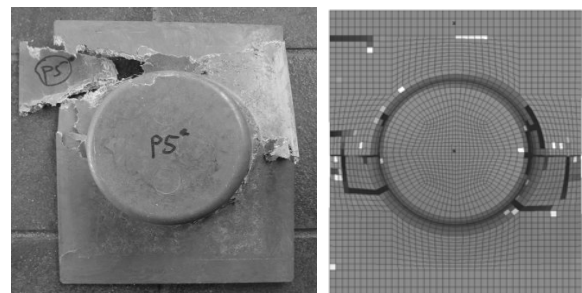


Fig.10. Comparison of the failure patterns: experimental vs. simulated (black elements have been eliminated) (100 mm/s)

As shown in Fig. 9, the predicted force-displacement curve, whilst certainly demonstrating a similar trend and failure profile, still yields some discrepancy when compared to the experimental results. The differences in the peak loads could be attributed to the complex mixed buckling-progressive bending mode of failure of the thin-walled component. Buckling of the flat portion of the prototype occurs at the initial stage of loading [9]. Further deformation process involves combined post-buckling bending and progressive folding of the component, which is concluded by the fracture development. This might point to a need for experimentation with regard to primary material characterisation to be more closely investigated and refined, so that a fair level of confidence in the exact evaluation and definition of the model parameters is

justified. Another area of investigation would be to accommodate the characterisation of the material by both tensile and compressive stress-strain curves in the analysis. This would include the replacement of von Mises failure criterion with the condition that would take into account the differences in the material strength parameters under tension and compression. In the example presented here, failure is characterised solely on the basis of the compressive failure mode, which may not be indicative of the failure pattern in those elements that fail due to a tensile load.

The comparison of the deformation and fracture modes and patterns experimentally recorded (video data) and obtained from the simulation (Fig. 10) shows good agreement. The simulation results show the model's ability to track crack growth and propagation. As can be seen, the failure pattern is accurately predicted at the regions situated near to the wheel well base and the areas adjacent to the clamps.

**4 Damage progression caused by low velocity impact**

Testing and simulation at higher crushing speeds is required in order to model the behaviour of the material in the low velocity impact loading (e.g. an automotive crash situation). The simulation has been performed for a 1000 kg added mass impact loading. The mass has been dropped at speeds of 1 and 5 m/s onto the prototype in the same direction as for the progressive crushing discussed in the previous section. Both approximations of the upper tensile and compressive stress-strain curves (with no residual stress included) were used. The analysis has been set up in PAM-CRASH by constraining the movement of the nodes on one edge of the prototype while adding mass and initial velocity to the nodes on the other edge. The force-displacement curves and failure modes are shown in Figs. 11 - 13.

The two analyses (A and B) have been performed using differing force-displacement curves and failure modes. The peak load predicted on the basis of the compressive stress-strain curve approximation (analysis B) is substantially higher at both speeds. The catastrophic failure point for the tensile stress-strain curve approximation (analysis A) is reached early due to application of the impact load, thus causing the peak load to be low.

The modes of failure progression predicted by both analyses (A and B) are shown in Figs. 12 -13. The finite elements shown in black colour have been eliminated and the elements shown in light colour

have almost failed. According to the analysis B the structure can withstand higher level of stress and strain, thus being able to support a higher load. This apparently provides more accurate projection of the material's behaviour under the impact loading under consideration.

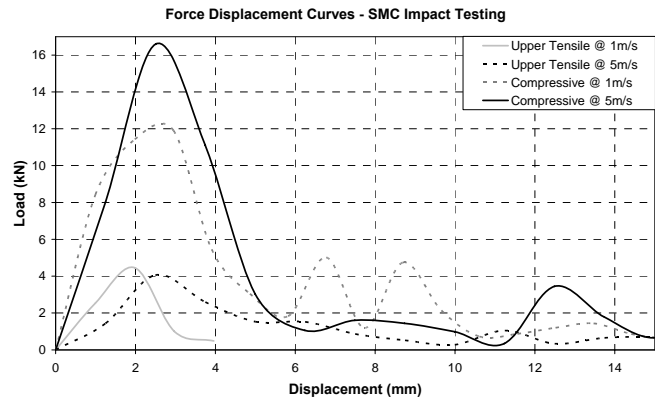


Fig. 11. Simulation of impact loading at 1 and 5 m/s

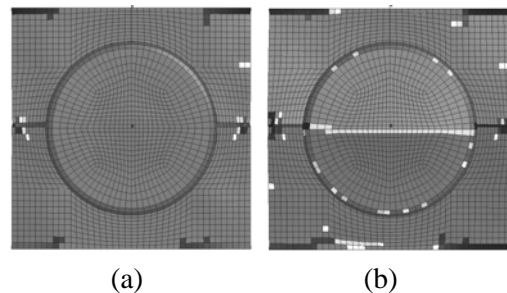


Fig.12. Analysis A: (a) initial failure; (b) progression of cracks

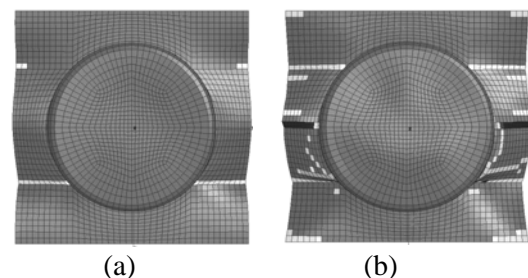


Fig.13. Analysis B: (a) initial cracking; (b) failure

The failure modes are similar in that the final failure cracks occur midway up the component on either side of the wheel well. The difference is that in the case A, initial failure also occurs on the impacted and constrained edges (Fig. 12a), and the cracks in the middle propagate over the wheel well

at final failure (Fig. 12b). In the case *B*, initial cracking occurs below the wheel well (Fig. 13a), whereas some damage does occur at the impacted and constrained edges (Fig. 13b). These results could serve as a benchmark in future testing and simulation.

## 5 Conclusions

The numerical modelling approach to the simulation of the damage evolution in thin-walled SMC composite components with complex shape and geometry based on the direct approximation of the experimental strain-stress curves has been developed. The corresponding algorithm was implemented into explicit finite element code (PAM-CRASH, ESI).

The performance of the developed SMC progressive damage model and algorithm in simulating the crush test is satisfactory considering the simplicity and practicality of the material characterisation procedure. The more extensive material characterization would probably enable further improvement and enhancement of the proposed modelling technology. The comparison of predictions to the experimental results shows that the developed model is able to describe the behaviour of SMC thin-walled structures at the beginning of the loading phase. Failure patterns showed promising similarity to that of the experimental failures. The use of the compressive stress-strain curve approximation produced considerable improvements in the profile of the force-displacement curves over the tensile stress-strain curve approximation, pointing to the need to develop the model based on both compressive and tensile failures. This would include the utilization of the failure criterion that takes into account the differences in the material strength parameters under tension and compression. Future versions of the progressive damage model would seek to take into account the sustained compressive strength of the material after failure.

## References

- [1] Mamalis A.C., Manolakos D.E., Demosthenous G.A. and Ioannidis M.B. “Crashworthiness of composite thin-walled structural components”, Technomic, 1998.
- [2] Hoffman L., Kabelka J. and Ehrenstein G.W. “Damage process modeling on SMC”, *Proceedings of the 10<sup>th</sup> Int. Conf. on Composite Materials (ICCM-10)*, British Columbia, Canada, Vol. 1, pp 335-342, 1995.
- [3] Meraghni F. and Benzeggagh M.L. “Micro-mechanical modelling of damage mechanisms in randomly oriented discontinuous fibre composite”. *Proceedings of the 10<sup>th</sup> Int. Conf. on Composite Materials (ICCM-10)*, British Columbia, Canada, Vol. 1, pp 487-494, 1995.
- [4] Desrumaux F., Meraghni F., and Benzeggagh M.L. “Generalised Mori-Tanaka scheme to model anisotropic damage using numerical Eshelby tensor”. *J. of Composite Materials*, Vol. 35, No. 7, pp 603-624, 2001.
- [5] Coutellier, D. and Rozycki, P. “Multi-layered multi-material finite element for crashworthiness studies”. *Composites: Part A*, 31, pp 841-851, 2000.
- [6] Morozov E.V., Morozov K.E. and Selvarajalu V. “Progressive damage modelling of SMC composite materials”, *Composite Structures*, 62, pp 361-366, 2003.
- [7] Morozov E.V., Kaczmarczyk S., Morozov K.E. and Selvarajalu V. “Numerical simulation of the progressive failure of SMC composite materials”. *Proceedings of the 14<sup>th</sup> Int. Conf. on Composite Materials (ICCM-14)*, San Diego, USA, 8p, (CD-ROM), 2003.
- [8] Morozov E.V. and Douglas J.A.S. “Progressive failure modelling of thin-walled short-fibre reinforced composite structures”. *Proceedings of the II ECCOMAS Thematic Conference on Smart Structures and Materials*, Lisbon, Portugal, July 18 – 21, (CD-ROM), 2005.
- [9] Morozov E.V. and Douglas J.A.S. “Progressive damage model development and failure simulation of the thin-walled structures made from SMC composites”. *Proceedings of the 6<sup>th</sup> Int. Conf. on Composite Science and Technology (ICCST/6)*, Durban, South Africa, January 22-24, (CD-ROM), 2007.